Soft Matter

Rheological properties and failure of alginate hydrogels with ionic and covalent crosslinks

Journal:	*Soft Matter*
Manuscript ID	SM-ART-05-2019-001039.R1
Article Type:	Paper
Date Submitted by the Author:	05-Sep-2019
Complete List of Authors:	Hashemnejad, Seyed Meysam; Mississippi State University, Chemical Engineering Kundu, Santanu; Mississippi State University, Chemical Engineering

Journal Name

ARTICLE

Rheological properties and failure of alginate hydrogels with ionic and covalent crosslinks

Received 00th January 20xx,
Accepted 00th January 20xx

DOI: 10.1039/x0xx00000x

www.rsc.org/

Seyed Meysam Hashemnejad,[a]† and Santanu Kundu [a]*

Polysaccharide-based hydrogels are being used in a wide variety of applications ranging from tissue engineering to food products due to their biocompatibility and the ease of gel formation. In real-life applications, hydrogels can undergo large strain deformation, which may result in structural damage leading to failure. Here, we report the nonlinear rheological properties and failure behavior of alginate hydrogels, a class of polysaccharide hydrogel, synthesized via ionic and covalent crosslinking. Gels with ionic crosslinks or ionic alginate hydrogels are prepared by addition of Ca^{2+} ions in the aqueous solution of sodium alginate, and the covalently crosslinked alginate gels or chemical alginate hydrogels are obtained via amidation reaction. Because of their structural difference, ionic and chemical alginate hydrogels display different scattering profiles captured by using small angle X-ray scattering (SAXS) technique. Both ionic and chemical alginate hydrogels exhibit strain stiffening behavior when subjected to large amplitude oscillatory shear (LAOS) and the strain-stiffening behavior is accompanied by negative normal stress. A custom-built cavitation rheometer has been utilized to probe the local failure behavior of these gels. The cavitation rheometry captures different defect growth or fracture mechanism in ionic versus chemical alginate hydrogels, even if these two types of gels have a similar linear elastic modulus. Based on the critical pressure for gel fracture, we have provided an estimate of the critical energy release rate.

Introduction

Hydrogels are crosslinked polymer networks which retain a large amount of water (as high as 99%) in their 3D structure. Interestingly, despite the presence of a considerable amount of water, hydrogels behave like elastic solids. Due to their unique physicochemical properties, the hydrogels have been extensively utilized in a wide range of applications ranging from transdermal delivery devices to the novel biomedical materials.[1–4] Hydrogels are prepared either from synthetic or natural polymers, and small molecule gelators. They can be formulated to meet the desired elastic and interfacial properties for a particular application. Despite significant advances in the rational design of the hydrogels, our understanding of their complex nonlinear mechanical response is limited.

Biological gel-like materials, containing semiflexible to rigid biopolymer chains, display unique nonlinear mechanical properties such as strain-stiffening behavior when subjected to the simple-shear deformation. The strain-stiffening for these biological gels commonly onsets at relatively low strain amplitude (γ_0).[5–7] For example, in the case of actin and collagen gels, strain-stiffening behavior is evident at $\gamma_0 \approx 0.1$. In contrast, polyacrylamide gels, a class of synthetic gels with more flexible polymer chains, exhibit strain-softening behavior.[8] The observed macroscopic strain-stiffening response has been linked to the chain bending at the moderate strain and chemical bond stretching at the larger strain values.[5,9] Additionally, strain-stiffening biopolymer gels often exhibit negative normal force during the simple-shear deformation (i.e., gel shrinks orthogonal to the shear direction).[6–8] Apparently, this behavior is critical for preserving the mechanical integrity of the extracellular matrix, such as in collagenous tissues.[10] In contrast, most synthetic gels with flexible chains display positive normal stress in shear deformation mode. It has been hypothesized earlier that the semiflexible chains subjected to tension and compression (orthogonal to each other) display different mechanical responses, stiffening vs. buckling. Such anisotropic response has been attributed to the negative normal force in shear deformation mode.[8] The origin of negative normal stress is still an open question, as other theories have also been presented.[8,11–13] The recent theoretical approach introduces the concept of tensegrity to the biopolymer networks. Based on this theory, the networks are stable when the chains are under tension (pre-tension), and such pre-tension dictates the modulus and nature of the normal force. [12] It has been predicted that for the swollen gels in a good solvent, the magnitude of normal stress in the simple-shear experiments is also governed by the sample aspect ratio.[13]

Alginate is a polysaccharide polymer extracted from brown algae. Alginate gels are extensively used in biological systems due to their low degree of cytotoxicity and easy gelation

[a] Dave C. Swalm School of Chemical Engineering, Mississippi State University, MS State, Starkville, Mississippi 39762, USA. E-mail: santanukundu@che.msstate.edu
† Present address: Department of Chemical Engineering, Massachusetts Institute of Technology, Cambridge, MA 02139, USA.

Electronic Supplementary Information (ESI) available: ionic gelation mechanism; gelation as a function of time; shear-moduli as a function of strain amplitude for ionic alginate gels; estimated Chebyshev coefficients and their rations; shape of cavities in cavitation experiments for ionic hydrogels. See DOI: 10.1039/x0xx00000x

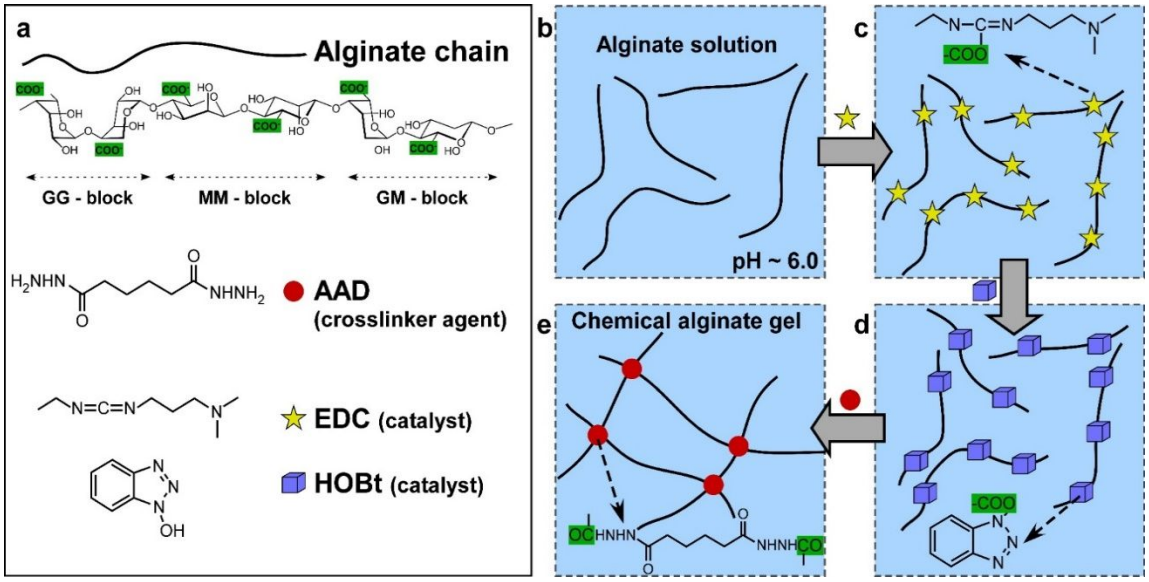

Figure 1 Schematic of chemical alginate synthesis process. **a** Chemical structure of the different compounds used in the reaction. **b** Alginate stock solution prepared in the buffer solution with pH of 6. **c** Addition of EDC activates the carboxylic functional groups on the alginate chains. **d** Addition of HOBt to further activate the carboxylic groups. **e** 3D structure of the chemical alginate gel by addition of the crosslinker agent, AAD.

process.[2,14] The polymeric alginate chain contains two monomers, mannuronic acid (M) and guluronic acid (G). The M and G monomers have similar compositions but different stereochemistry (Figure 1a). The aqueous solution of alginate can be transformed into hydrogels via either ionic or chemical crosslinking. Ionic alginate gel can be formed in the presence of multivalent cations such as Ca^{2+} (Figure S1). Such gelation occurs through either a fast or slow gelation method. The fast gelation process is achieved by using a highly water-soluble calcium compound, e.g., $CaCl_2$. This is typically performed by dripping alginate stock solution into a high concentration $CaCl_2$ solution. The slow gelation, used in this work, utilizes a sparsely water-soluble calcium salt (at neutral pH), $CaHPO_4$. The calcium salt solubility is typically enhanced by lowering the pH.[7] It has been reported that the ionic gelation is mainly promoted through ionic interaction between GG units and cations.[15] Multiple GG units associate with Ca^{2+} ions to form junction zones. These junction zones act as crosslinks in ionic alginate gels.

In addition, alginate gels can be obtained via a chemical reaction between the carboxylic groups of the alginate chains and water-soluble crosslinker agents consisting of multiamine functional groups.[16] To promote the amidation reaction in water, a catalyst agent is often required.

In this article, the nonlinear rheological properties of ionic and chemical alginate gels are reported, which are determined using shear and cavitation rheology techniques.[17–23] Cavitation rheology has become an important tool to study the local mechanical properties and fracture behavior of soft gels. This method involves pressurizing a pre-formed defect using a syringe needle. The system pressure is monitored as a function of time and at a critical pressure, P_c, the defect grows rapidly either in the form of elastic cavitation or the material undergoes irreversible fracture. This sudden material expansion caused a rapid decrease in system pressure. For a cavitation process P_c scales with the local elastic modulus of the material. Additionally, in a fracture event, P_c provides information regarding the critical energy release rate, G_c.[18]

We recently reported nonlinear rheological behavior of ionic alginate hydrogels in a simple shear mode.[7] However, such rheological results have not been reported in details for the chemical alginate gels. This motivates us to investigate the nonlinear rheological behavior of chemical alginate gels and compare the results with that obtained for the ionic alginate gels. In addition, cavitation rheology allows us to examine the local failure mechanism of these gels.

Materials and methods

Material

N-(3-Dimethylaminopropyl)-N′-ethylcarbodiimide (EDC), 1-Hydroxybenzotriazole hydrate (HOBt), adipic acid dihydrazide (AAD), 2-(N-Morpholino)ethanesulfonic acid (MES), NaOH, calcium phosphate ($CaHPO_4$), and glucono delta-lactone (GDL) were purchased from Sigma-Aldrich (St. Louis, MO). Sodium alginate (with G block mole fraction of G/ (G+M) ~ 0.78) and M_w ~ 260,000 g/mol (Protananal LF 20/40) was kindly provided by FMC Technologies. DI water with a resistivity of ~ 18.2 mΩ was used for the preparation of the alginate gels. All the chemicals were used as received.

Gel formation

Chemical alginate gels were prepared using the amidation reactions (Figure 1).[16] Activation of carboxylic functional groups in alginate chains were carried out in two steps, EDC was added first, followed by HOBt. The reaction was conducted in the

buffer solution at pH = 6.0. The buffer solution was prepared by the addition of an appropriate amount of NaOH solution into MES solution (final MES concentration was 0.1M). The pH of the reaction media was selected to be in the range required for carboxylic activation reaction and higher than pKa of the primary amine in AAD (pKa ~ 2.5) to avoid the presence of unreactive protonated amine groups (NH_3^+). Alginate stock solution (1% wt.) was prepared by mixing alginate powder in the buffer solution using an overhead mixer (Troemner LLC) and was mixed at 1000 rpm. Next, EDC followed by HOBt were then added and was mixed for one hour. An equimolar amount of EDC and HOBt was selected with respect to the carboxylic acid group present in the system. Lastly, the desired amount of crosslinker (AAD) was added into the solution and was mixed for an additional 1 min before being transferred either in 20 mL glass vials or between plates of a rheometer. In order to compare the rheological behavior of chemical and ionic alginate gels in a systematic manner, we have maintained the concertation of the crosslinking agent, AAD, similar to calcium concentration in ionic alginate gels reported in our previous publication.[7] Interestingly, the linear shear moduli obtained for chemical alginate gels are similar to the ionic alginate gels when a similar concentration of either AAD or calcium ions are used.
As discussed in details earlier, ionic alginate gels (1% wt.) were prepared by addition of the sparsely water-soluble calcium compound, $CaHPO_4$.[7] Given amount of the calcium phosphate ($[Ca^{2+}]$ = 10 mM, 12.5 mM, and 15 mM) was added in the alginate stock solution and was mixed for 5 minutes. Lastly, GDL (GDL/ $CaHPO_4$ = 3 mol/mol) was added followed by mixing for an additional 30 s. The solution was then either transferred into a rheometer or glass vials for gel formation.

Shear rheology

A stress-controlled rheometer (HR2, TA Instruments) was used for rheological characterization. A 20 mm parallel plate geometry with solvent trap was used. Adhesive-backed sandpaper (grit # 60) was attached to both upper and lower plates to minimize slippage at the gel-geometry interfaces. The gap between the plates was kept at 1.5 mm unless otherwise mentioned. Time sweep experiment was performed to capture the gel formation in situ on the rheometer (strain amplitude, γ_0 = 0.1% and angular frequency, ω = 1 rad/s). Subsequent to the gel formation, the frequency sweep tests (at γ_0 = 0.1% and ω = 0.1 rad/s - 20 rad/s) and strain sweep tests (at ω = 0.5 rad/s γ_0 = 0.1%-300%). Raw stress-strain signals were analyzed using MITlaos software.[24] All rheological measurements were conducted at room temperature). The stress-strain data affected by the cohesive gel failure or slippage at the gel-plate interface (adhesive failure) have not been considered for data analysis. Negative normal force (NNF) and torque signals were collected separately using auxiliary data logger software provided by TA Instruments.

Cavitation rheology

A custom-built cavitation rheometer set-up was used, as discussed in our earlier publication.[19] The gel samples (cast in 20 mL glass vial) was secured on a movable stage (with standard micrometers providing XYZ translation) and then vertically moved upward to insert the needle (24 gauge, Metal Hub NDL, 2 in, point style 3 from Hamilton) into the gels. Prior to cavitation rheology measurements samples were stored overnight. A 60 mL syringe was used for system pressurization. The pumping speed was controlled using a programmable syringe pump (New Era). The pumping rate was kept fixed at 5 mL/min. A pressure transducer (Px26 series, Omega Engineering) was used to record the gauge pressure of the system during the pressurization process. Either a digital 20 fps camera (Basler) or a high-speed camera (M310, Vision Research) was mounted on an XY translation stage to capture the gel deformation at the tip of the syringe needle inside the gels. The cavitation experiment was controlled by a program written in the LabVIEW software. The measurements were repeated at least five times to report the average P_c and standard deviation.

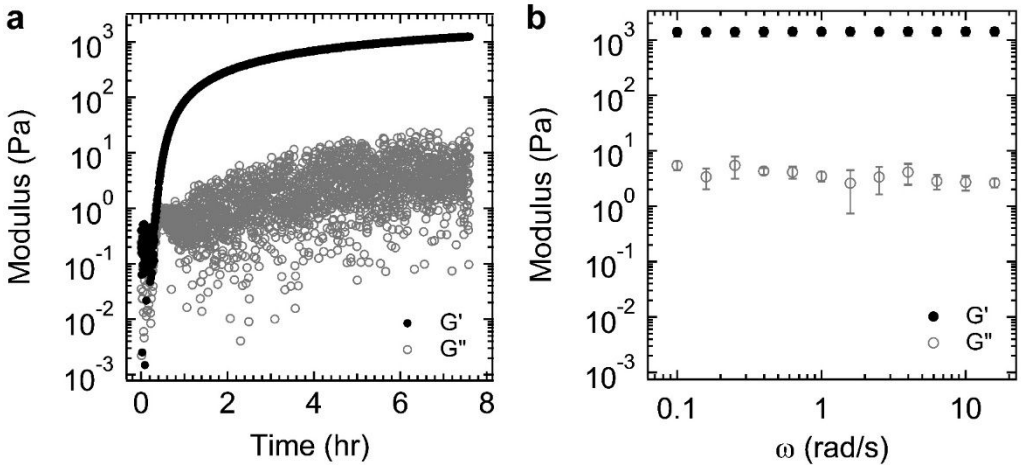

Figure 2 *In situ* gelation of chemical alginate on a rheometer. **a** Evolution of shear viscoelastic moduli measured at strain amplitude γ_0 = 0.1% and ω = 1 rad/s. **b** Results from frequency sweep experiment after gel formation. Concentration of alginate is 1 % wt. and [AAD] = 12.5 mM.

Small angle X-ray scattering

The scattering experiments were performed by a staff scientist at the Argonne National Lab.[25] The samples were loaded in quartz capillary with a nominal outer diameter of 1.5 mm (Hampton Research Corp.), and a wall thickness of 0.01 mm. Igor Pro 6.37 was used for the fitting. The desmeared scattering data were used for the fitting with an appropriate model, as discussed below.

Results and Discussion

Gel formation

The sol-to-gel transition was investigated *in situ* in a rheometer by monitoring the evolution of the viscoelastic properties. Figure 2a displays the first-harmonic storage (G') and the loss moduli (G'') as a function of time for the chemical alginate gel, obtained from a time-sweep experiment. As the gelation progresses, G' sharply rises during the first hour and then gradually increases until reaching an apparent plateau. At the plateau region, G' becomes two orders of magnitude higher than G'', indicating the completion of the gelation process. Figure 2b displays the results from the frequency sweep experiment performed on the formed gel. G', G'' are nearly independent of frequency over more than two decades of frequency, further supporting the gel-like behavior of the sample. In addition, gelation time – the time at which an apparent plateau in G' is reached in the time-sweep experiment– is correlated with the crosslinker concentration. For example, gelation time has been ~ 7 hr for the gel with [AAD] = 12.5 mM and the time increases to ~ 10 hr for [AAD] = 10 mM (Figure S2).

Similarly, the evolution of G' and G'' were monitored for ionic alginate gels on a rheometer, as reported previously (also shown in Figure S2).[7] A distinctly different gelation kinetics can be observed for the ionic alginate gel in comparison to the chemical one. The initial increase of moduli is faster in the chemical alginate (Figure S2). This may be due to the slow hydrolysis process of the GDL in the solution and the corresponding gradual release of Ca^{2+} ions in the solution. Ca^{2+} crosslinks the alginate chains (ionic bonds with the carboxylic groups) to form a gel. However, the final gelation time in ionic alginate gels is comparable to that observed for the chemical alginate gels for a similar concentration of crosslinker agents.

Gel structure

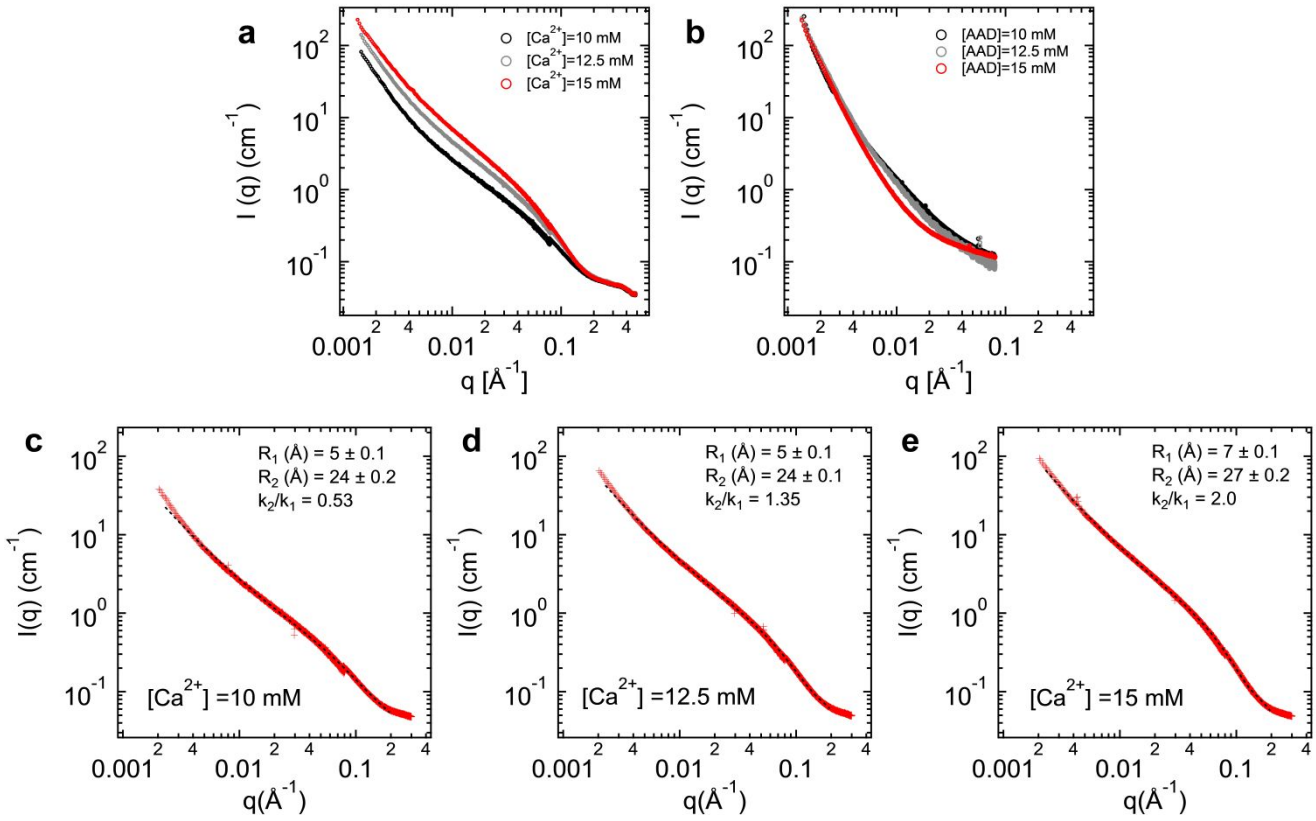

Figure 3 Small angle X-ray scattering data (scattering intensity, *I(q)* versus scattering vector, *q*) obtained for ionic (**a**) and chemical (**b**) alginate gels with different crosslinker concentration. The data for ionic gels, shown in **a**, are used for the model fit and are shown in: **c** $[Ca^{2+}]$ = 10 mM, **d** $[Ca^{2+}]$ = 12.5 mM, and **e** $[Ca^{2+}]$ = 15 mM. Dotted lines in **c**, **d**, and **e** correspond the model fit to the experimental data. The polymer concentration is 10 mg/mL. The intensity error has been considered in the fitting.

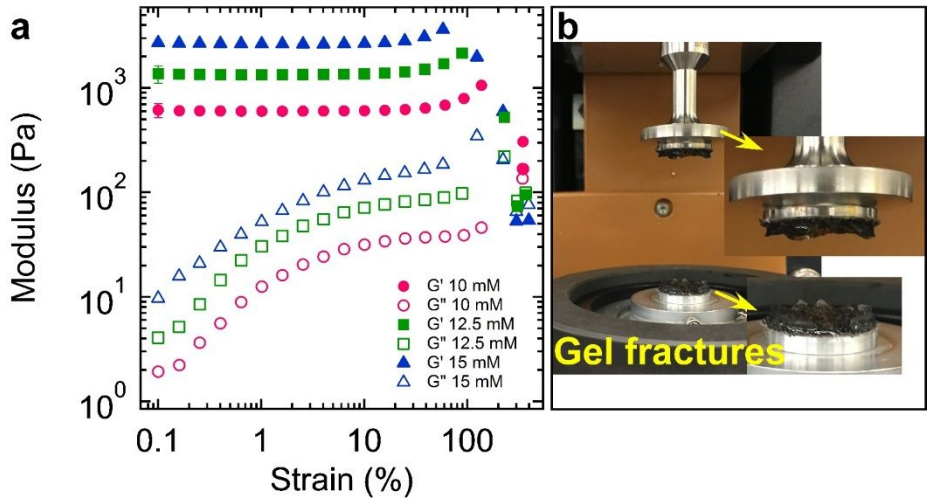

Figure 4 Strain stiffening and fracture behavior of chemical alginate gels subjected to oscillatory shear. **a** LAOS measurements for the crosslinker (AAD) concentration of 10 mM, 12.5 mM, and 15 mM. **b** Images of cohesive fracture of the gel subjected to large strain (strain amplitude = 300%). Concentration of alginate is 1 wt. % in all cases. The error bars represent one standard deviation.

Structure of the ionic and chemical alginate gels was investigated using the small angle X-ray scattering (SAXS) as a function of Ca^{2+} and AAD concentration (Figure 3). A noticeable scattering difference is observed between ionic and chemical alginate gels. The scattering intensity, *I(q)* as a function of scattering vector, *q* for the ionic alginate gels increases as the Ca^{2+} concentration increases from 10 mM to 30 mM, particularly for $q < 0.2$ Å^{-1}. In contrast to the ionic alginate gels, the scattering profiles of the chemical alginate gels do not display such a clear distinction with the change in crosslinker (AAD) concentration. As presented in Figure 3b, the scattering intensity increases with decreasing q and nearly overlaps for the AAD concentration of 10 mM to 30 mM. The scattering results for the chemical alginate gels indicate that the microstructure does not change significantly with increasing crosslinker concentration, as expected from the free-radical polymerization process.

Increasing the Ca^{2+} concentration in the alginate solution results in an evolution of the junction zone structure. This may include the formation of new junction zones, an increase in the length of the previously formed junction zones, growth of the junction zone diameter, or a combination of these events. However, an increase in scattering intensity of ionic alginate gels as a function of Ca^{2+} is often correlated with the growth of junction zone diameter. [26,27] To quantify this structural change in ionic alginate gels, the scattering results are fitted with a model, as described below. Junction zones can be considered as rods, as these zones are relatively stiff in comparison to the more flexible alginate strands between the junction zones. Therefore, the form factor for broken rods has been used to describe the junction zones in the ionic alginate gels, as described by Yuguchi et al.:[26,27]

$$I(q) = \frac{1}{q^2}\left[\sum_{i=1}^{2} k_i q \left[\frac{J_1(qR_i)}{qR_i}\right]^2 + k\right]$$

Where, J_1 is the first-order Bessel function, R_i is radius of the i^{th} rod, and *k* and k_is are the adjustable constants. The junction zones are most likely polydisperse in size, but two rods with different radial dimensions of R_1 and R_2 can capture the scattering data adequately, i.e., *i*= 2 is considered here. k_2/k_1 is an estimated number ratio of the junction zones with radius of R_1 and R_2, respectively. Also, R_1 and R_2 capture the upper and lower bound of the junction zone radius. The summation term in the above equation captures the scattering behavior of the junction zones. Additionally, the k/q^2 term in the equation captures the other spatial correlations (specifically single strands polymer chain contribution) not considered by the broken rods.

The above model can fit the experimental data reasonably well. The estimated values for R_1, R_2, and k_2/k_1 are presented in Figure 3 for three different [Ca^{2+}]. The R_1 and R_2 values are found to be similar for [Ca^{2+}] of 10 mM and 12.5 mM. These values slightly increase for the 15 mM case. Additionally, R_1 values do not change with Ca^{2+} concentration. The fitting indicates that the minimum diameter of zunction zone is about 1 nm, which is equivalent to a junction zone formed by two strands.[28] R_2 values are fivefold that of R_1 (2.5 nm vs. 0.5 nm). The k_2/k_1 values increases with adding [Ca^{2+}] which signifies that the fraction of rod component with R_2 increases with respect to R_1. The junction zones dimensions obtained here are in the same range reported in the earlier publications, estimated for ionic alginate gels.[26,27]

Nonlinear mechanical properties

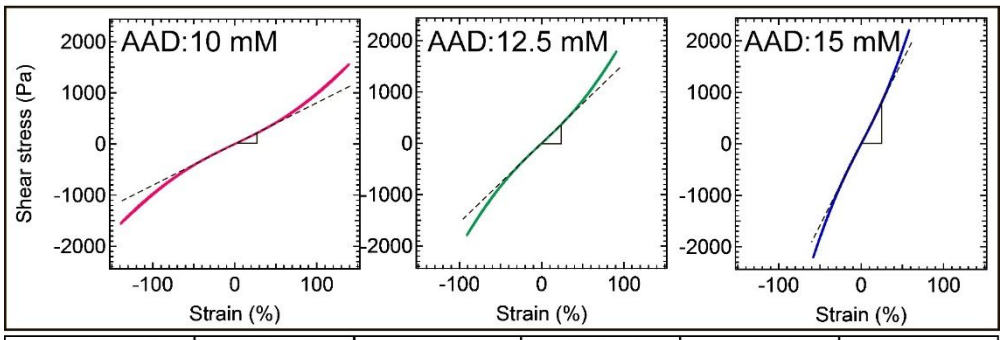

AAD (mM)	G'_1 (Pa)	G'_M (Pa)	G'_L (Pa)	e_3 (Pa)	G'_L / G'_M
10	1,048	764	1,118	79	1.47
12.5	1,870	1,493	1,967	106	1.32
15	3,638	3,062	3,790	165	1.24

Figure 5 Shear stress-strain (Lissajous-Bowditch) curves for chemical alginate gels with different concentration of AAD. Data correspond to the maximum strain amplitude that a sample can sustain during LAOS measurements, i.e., γ_0 ~ 140% for AAD = 10 mM; γ_0 ~ 90% for AAD = 12.5 mM; γ_0 ~ 60% for AAD = 15 mM. All measurements are conducted at ω = 0.5 rad/s. Dash lines corresponds to the linear elastic responses. Table presents different parameters obtained using MITlaos program.

After *in situ* gelation step in a rheometer, the formed hydrogels were subjected to the large amplitude oscillatory shear experiments. The elastic and viscous coefficients of the first harmonic component of Fourier series were recorded by the rheometer software. Figure 4a displays the first-harmonic storage (G') and loss (G'') moduli as a function of strain amplitude for the gels with different concentration of AAD. At small strain amplitude, an increase in G' with increasing AAD concentration has been observed, i.e., the gels become stiffer with increasing crosslinker concentration. Increasing [AAD] concentration, theoretically increases the number of the load-bearing polymer chains per unit volume in the crosslinked network resulting in higher modulus.

At the nonlinear regime (for example, at $\gamma_0 > 10\%$ for [AAD] = 15 mM), the chemical alginate gels show strain-stiffening behavior, where the G' increases with strain amplitude. The strain-stiffening behavior is similar to that previously reported for the ionic alginate hydrogels (also shown in Figure S3).[7] The drop in G' and G'' in chemical alginate gels beyond the strain-stiffening response is an indication of the material/gel failure. An image of a gel failed at a large strain amplitude ($\gamma_0 = 300\%$) is shown in Figure 4b. It is likely associated with the cohesive fracture of the hydrogels, i.e., breaking of covalent bonds in the network. Additionally, the samples sustain a relatively larger strain before failure with decreasing AAD concentration. For example, the maximum strain amplitude for the gels with [AAD] = 10 mM is ~140%, whereas for [AAD] = 12.5 mM and 15 mM, the maximum strain amplitude are recorded as ~ 90% and ~ 60%, respectively. At higher crosslinker concentration, the chain contour length between the crosslinking points decreases, correspondingly, the maximum chain extension decreases.

The failure behavior of the ionic alginate gels at large-strain is different, where the gel sample detaches from the upper fixture at higher strain amplitude. This can be attributed to the adhesive failure at the gel-plate interfaces.[7] Interestingly, we have noted an increase in G'' with increasing strain amplitude at the lower range of strain-amplitude considered here. With further increase in strain-amplitude, G'' reaches an apparent plateau. The origin of initial increase of G'' is not apparent at this stage and can be attributed to the non-crosslinked chains, but further investigation is needed.

To quantify the strain-stiffening behavior of the chemical alginate hydrogels, the intra-cycle stress-strain data was evaluated. Figure 5 displays the shear stress vs. strain (2D Lissajous-Bowditch curves) corresponding to the maximum strain amplitude prior to the gel failure. The shear stress is independent of the applied-strain direction, indicated by the overlap in the stress data measured from low to high strain, and the reverse. Almost absence of the viscous dissipation (no

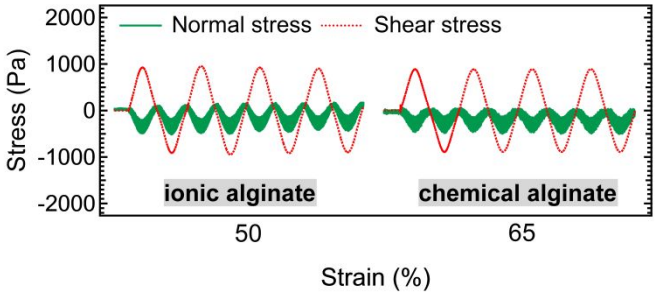

Figure 6 Negative normal stress (green) and shear stress (red) in oscillatory shear experiments for ionic and chemical alginate gels. Concentration of alginate is 1% wt and concentration of the crosslinking agent is identical for ionic and chemical alginate gels ($[Ca^{2+}]$ = 12.5 mM and [AAD] = 12.5 mM). Note that the strain-amplitudes are slightly different for these two gels necessary to compare the normal stress at the similar shear-stress.

significant hysteresis loop) in the Lissajous-Bowditch curves can

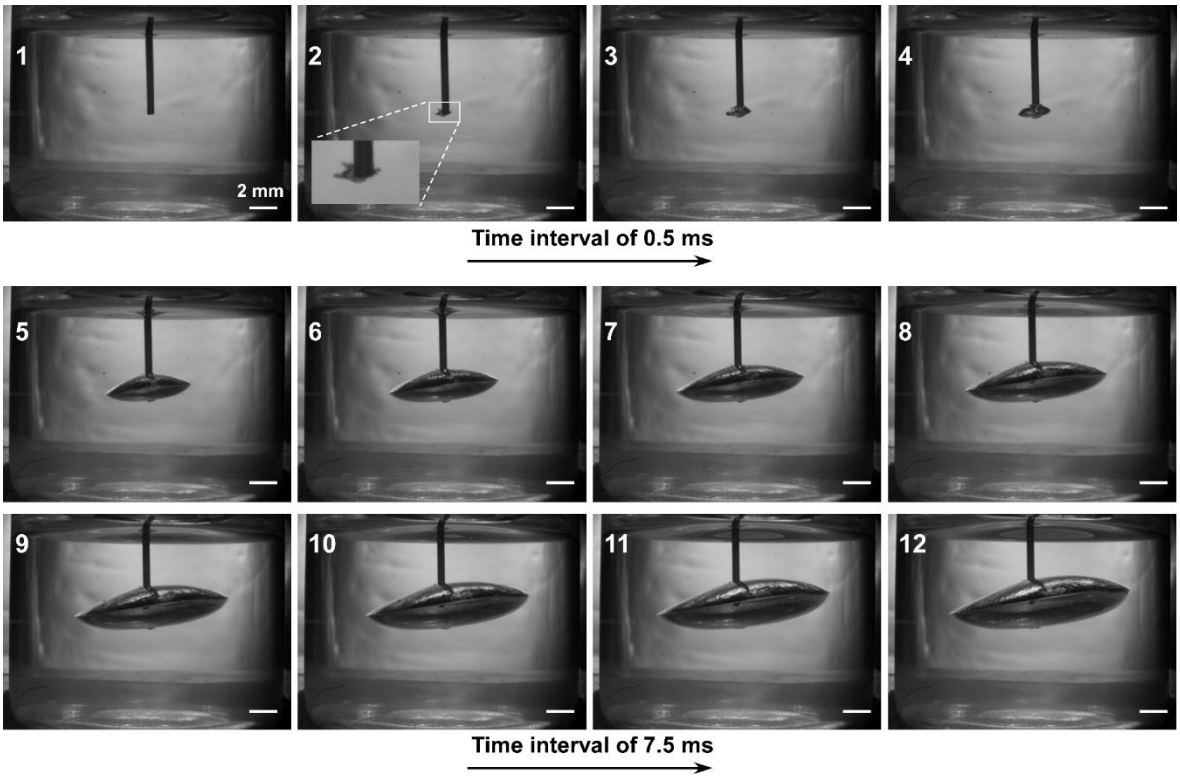

Figure 7 Time-lapsed images during fracture of ionic alginate gel, [Ca^{2+}] = 12.5 mM. The crack initiates in the frame number 2 followed by propagation into an ellipsoid shape. The time interval between the frames 1-4 is 0.5 ms, whereas that between the frames 4-12 is 7.5 ms.

be noted (Figure 5). The chemical alginate gels behave very much like an elastic solid even though the network contains ~ 99 wt% of water. This solid-like behavior is further supported by the frequency sweep data presented above (Figure 2b). Although low, the viscous contribution is more significant in the ionic alginate gels. Particularly, G'' in the ionic alginate gels is about one order of magnitude higher than that in chemical alginate gels, whereas, these gels have similar G' value (Figure S2). The higher values of loss modulus in ionic alginate gels are mainly due to the nature of ionic crosslinking. It has been previously reported that ionic alginate gels have relatively faster stress relaxation process in comparison to the chemical alginate gels, where the relaxation time can be as high as 1000 s.[29] This further supports the tightly crosslinked structure of the chemical alginate gels.

To quantify the nonlinearity in the rheological responses of chemical alginate gels, further interpretations of various moduli are presented in a table in Figure 5. Again, these results correspond to the maximum strain amplitude that the chemical alginate samples for different AAD concentrations can sustain. The minimum (tangent modulus, G'_M) and the maximum (secant modulus, G'_L) elastic moduli are estimated at γ = 0% and $\gamma = \gamma_L$ %, respectively.[24] G'_1 (or e_1) and e_3 are the first- and third-order Chebyshev polynomial coefficients, respectively. G'_1 is same as G' estimated by the rheometer software and is a measure of an average modulus throughout the oscillation cycle for a given strain amplitude.[24] The e_3 values as a function of strain amplitude for different AAD concentrations are shown in Figure S4a.

As reported in the literature, in the linear viscoelastic regime,[24] a uniform slope is observed throughout the elastic stress-strain curve, i.e., $G'_M = G'_L = G'_1$, and $e_3 \approx 0$. However, in the nonlinear regime, this equality is not seen and $G'_L > G'_M$ (also shown in G'_L/G'_M ratio) and $e_3 > 0$. An example of such responses is shown in Figure 5. The positive values of e_3 and $G'_L/G'_M > 1$ also confirm the intra-cycle stiffening behavior. The change of e_3 as a function of strain (Figure S4) clearly captures the onset of non-linearity in elastic responses. The onset takes places at lower strain amplitude with increasing AAD concentration. Also, with increasing crosslinker concentration we have been able to capture a higher extent of strain-stiffening.

In addition to e_3, we have estimated the e_3/G'_1 ratios (see Figure S4b) and both of these parameters can capture the onset of non-linearities. Comparing e_3/G'_1 for the chemical and ionic alginate gels at the crosslinker concentration of 12.5 mM (Figure S4c), we found that for the ionic alginate the onset of non-linearity takes place at a lower strain. Also, in the non-linear regime, e_3/G'_1 values for these gels are higher than that for chemical alginate gels, while G'_1 values are quite similar. Based on these observations, we can hypothesize that the ionic alginate displays more strain-stiffening behavior in comparison to chemical alginate gels.

We reported earlier that the ionic alginate gels display negative normal stress when the material is subjected to oscillatory shear.[7] We postulated that such an observed negative normal stress is related to the semiflexible nature of the alginate chains, particularly the strand between the junction zones. In addition, stiff junction zones can also attribute to the negative normal

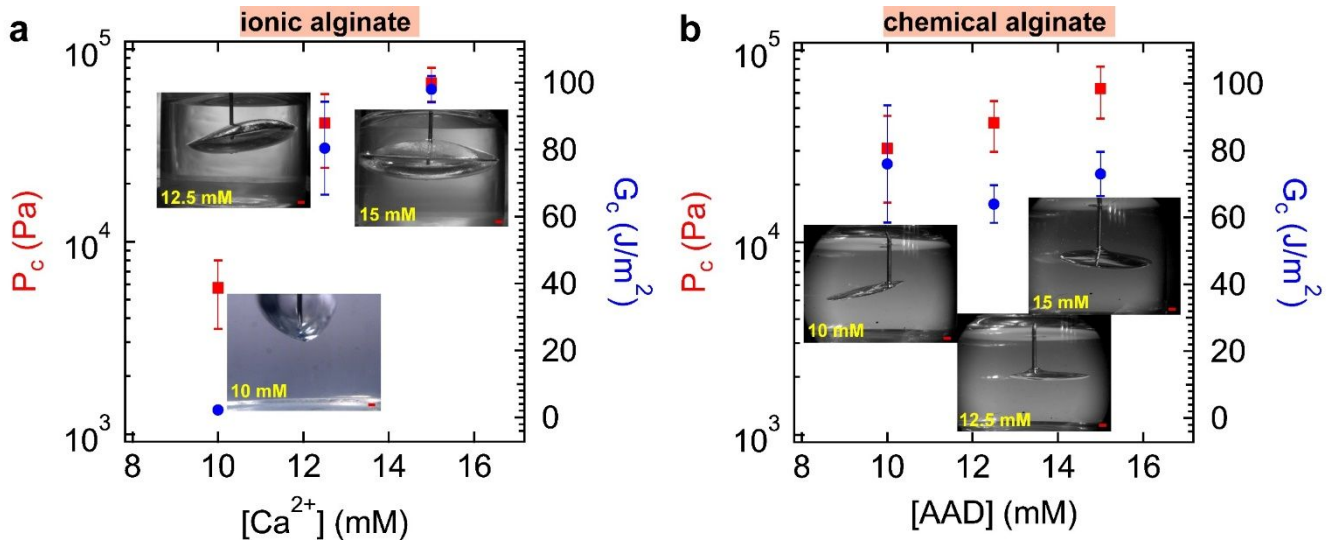

Figure 8 Cavitation rheology results as a function of crosslink concentration for **a** ionic alginate gels and **b** chemical alginate gels. Scale bar on the images represent 1 mm.

stress as those can be subjected to bending and stretching during oscillatory shear. Since junction zones are not present in chemical alginate gels, comparing the responses of ionic and chemical alginate gels provides better insights regarding the contribution of polymer strands versus junction zones in the observed negative normal stress. Figure 6 demonstrates the negative normal stress and shear stress in chemical and ionic alginate gels during multiple cycles of the oscillatory shear measurements. Interestingly, the negative normal stress values are similar for the ionic and chemical alginate gels, with similar shear stress values. Therefore, we can hypothesize that the observed negative normal stress is most likely related to the semi-flexibility of the alginate strands and the contribution of the bending and stretching of junction zones present in ionic alginate gels is not significant, particularly for the strain-values considered here. Further, in ionic alginate gels, as the gelation proceeds, during the *in situ* experiments, negative normal stress (~ -100 Pa) has always observed.[7] However, in chemically alginate gels, such initial normal stress was not found (or smaller than the detection limit of the instrument). Intriguingly, the effect of geometry on negative normal stress has been reported by Yamamoto et al. for the gels consisting of flexible chains.[13] However, for alginate gels, it requires further investigation to elucidate how geometry and aspect ratio of the gel sample affect the observed nonlinearity.

Fracture behavior through cavitation rheology

The cavitation rheology experiments were conducted to probe the fracture/failure behavior of alginate gels. An initial circular crack inside the gel was formed by inserting a flat-tip needle (ID: 310 μm and OD: 570 μm). The crack was then pressurized by pumping air into the system. Typical results for such experiments for ionic alginate gels is shown in Figure 7. Here, an ionic alginate gel with 12.5 mM Ca^{2+} concentration is considered. With pressurization, initially, the air-gel interface deforms slightly, then the crack slightly expands non-symmetrically (crack front moves into the bulk of the sample). This is followed by a rapid increase of the cavity volume. The shape of the generated cavity is ellipsoid in nature. Such a sudden increase in cavity causes a drop in pressure. The maximum pressure is defined as a critical pressure (P_c) for such sudden expansion. To capture such relatively fast incident (less than 1 sec), a high-speed camera, with 5000 fps, was used.

Interestingly, the shape of the growing defect in ionic alginate gels depends on the concentration of calcium ions. For example, in ionic alginate gels with [Ca^{2+}] = 10 mM, a spherical cavity is observed (Figure 8a, and Figure S5). By increasing [Ca^{2+}] to 12.5 mM, the failure mechanism is characterized by an ellipsoid-shaped fracture which grows horizontally. In contrast, the defect growth is mostly planar (almost no cavity) with an acute angle to the horizontal plane (Figure 8b).

Before approaching the critical pressure, P_c, the gel samples are stretched only to a very small strain (< 10%). The strain can be estimated from the stretch ratio (λ), which is defined as $\lambda = (A_c / A_{co})^{1/2}$, where A_c is the area of the spherical cap formed at the tip of the needle at the instability point, and A_{co} is the inner cross-sectional area of the needle. The strain the samples are subjected to lies in the linear viscoelastic regime, as measured in shear rheology. However, beyond P_c the defect grows to a strain which is higher than the maximum strain amplitude the gel network can sustain. It implies that the defect growth involves an irreversible failure of the network. Such behavior is different than the reversible, elastic instability observed in a few gels undergoing a large strain deformation.[18] Figure 8 summarizes the P_c and crack growth images in the ionic and chemical alginate gels as a function of crosslinker concentration. The nature of crack growth and the magnitude of P_c depend on the type and degree of crosslinking. In general, P_c increases with the crosslinker concentration, similar to the increase in G'. Such correlation between P_c and G' have been reported for different gel systems.[17–20,30] The increase of P_c is more prominent for the ionic alginate gels.

The shape of fracture/defect growth can be discussed in the context of different crosslinking mechanism. We hypothesize that in the ionic alginate gels, the progression of fracture plane (shown in Figure 7) involves dissociation of junction zones present in the system rather than breaking of covalent bonds.[28] The spherical cavity growth in ionic alginate gel with [Ca^{2+}] = 10 mM (Figure 8a) is linked to the relatively weak gel structure, containing mostly unsaturated GG blocks (less number of junction zones) and lower modulus. In the chemical alginate gels, however, we postulate that the stored elastic energy in the chains between the crosslinking points is released at P_c by breaking of covalent bonds. The shape of the crack growth (2D fracture plane) in the chemical alginate gels is similar to the fracture occurs in a brittle solid. This is in agreement with nearly pure elastic behavior of chemical alginate gels, captured in shear rheology, where G' is about 2 orders of magnitude higher than G''.

Since the cavitation rheology captures fracture like behavior, critical energy release rate (G_c) can be estimated from the P_c values. G_c is defined as the energy needed to create a unit surface area during a fracture incident. For most gel-like material with single polymer network, G_c has been reported in the range of 1-100 J/m^2,[31–34] and in the molecular gels, G_c is estimated to be ~ 0.1 J/m^2.[21] These values are obtained from various experiments including cavitation rheology. G_c can be correlated with P_c as $G_c \approx \frac{P_c^2 r_s}{\pi G'}$, where r_s is the inner needle radius.[18,35] It should be noted that the above formula is based on the linear fracture mechanism, i.e., fracture occurs at a small strain. As plotted in Figure 8, G_c, increases in ionic alginate gels with [Ca^{2+}], whereas it remains relatively unchanged in chemical alginate gels with different [AAD].

We used the classical Lake-Thomas (LT) theory developed for predicting the energy release rate for rubbery materials, to further elucidate the fracture process in the alginate gels.[36] For the chemical alginate gel, where the fracture process involves chain scission (bond breaking), G_C can be estimated based on the LT theory as $\sim NU\Sigma_0$. Here, N is the degree of polymerization of an alginate chain connecting two crosslinking points, U is the bond energy, and Σ_0 is the areal chain density. We assume that the during fracture the scission of glycosidic bonds connecting the saccharide units take place. The bond energy of the glycosidic bond is $U_{C\text{-}O} \approx 360$ kJ/mol. Also, $\Sigma_0 \sim 1/\xi^2$, where ξ is the mesh size. Mesh size for our system can be estimated as $\xi \sim (k_B T/G')^{1/3}$.[28] k_B is the Boltzmann constant, T is the temperature. For the [AAD] = 10 mM, 12.5 mM, and 15 mM, we estimate $\xi \sim$ 15.7 nm, 13 nm, and 10.3 nm, respectively. It is difficult to determine the chain length (therefore, the value of N) between the croslinking points for our case. But we can assume that chain length (contour length) of the semiflexible alginate chain connecting two crosslinking points is $\approx \xi$. Considering the length of each monomeric unit is ≈0.9 nm, from ξ, we obtain $N =$ 18, 15, 12 for the [AAD] = 10 mM, 12.5 mM, and 15 mM, respectively. Using these values, we estimate $G_c \sim$ 0.04, 0.05, 0.07 J/m^2, respectively.

Similar estimation for G_C can be conducted for the ionic alginate gels. For these samples, the fracture process involves unzipping of junction zones. Here, G_C can be presented as $\sim L_J U_I \Sigma_{0J}/l$. Here, U_I is the ionic bond energy, L_J is the length of the junction zone, l is the length of one binding unit, and Σ_{0J} is the areal density of junction zones. From the density functional calculations (DFT) it has been shown that $U_I \approx$ 3.5 eV (≈ 330 kJ/mol) with and without the presence of the water molecules.[37] However, if the Ca^{2+} ion is considered to be hydrated, then U_I becomes ≈ 2 ev (≈ 190 kJ/mol).[37] On the other hand, Baumberger and Ronsin considered $U_I \approx 12 k_B T$ (≈ 30 kJ/mol),[28] estimated based on the Bjerrum length. If the ionic bond energy (U_I) is of the same order of covalent bond energy (U), the unzipping of junction zones is not likely and further simulation/theoretical study is necessary to elucidate that further. For our estimate, we have considered, $U_I \approx 100$ kJ/mol, somewhere in between the highest and lowest U_I values noted above.

In our case, $l \sim 0.9$ nm,[28] however, we have not been able to experimentally determine the magnitude of L_J, as the SAXS experiments only provide information regarding the diameter of the junction zones, but not the length of those. Literature report indicates that gelation is possible if the number of binding units per junction zone is at least 20 and we have considered this number for our estimation. In other words, we have $L_f/l \sim 20$.[7,38] Similar to chemical alginate gels, we estimate $\Sigma_{0J} \sim 1/\xi^2$ and $\xi \sim (k_B T/G')^{1/3}$.[28] We estimated $\xi \approx$ 18 nm, 16 nm, 12 nm, for the [Ca^{2+}] of 10 mM, 12.5 mM, and 15 mM, respectively. Using these values, we estimate $G_c \sim$ 0.01, 0.013, 0.023 J/m^2, respectively. If $L_f/l > 20$, signifying the increased length of junction zones, the estimated G_c value will change, but is expected to be the similar order of magnitude.

Several observations can be made regarding the experimentally determined and theoretically estimated G_c. For ionic alginate gels, the G_c values are an order of magnitude higher than that determined by Baumberger and Roslin using a custom-built setup.[28] We hypothesize that this is because of different fracture geometry used here. Also, it may be possible that the gel sample just below the needle is pre-stressed because of needle insertion and this can result in higher critical pressure. In a previous simulation study, we have shown that the presence of a solid boundary can increase the critical pressure significantly.[20] This will be further investigated in a future study. Also, the theoretically estimated G_c values are almost three orders of magnitude lower than the experimentally observed values. Such difference has also been observed by Baumberger and Roslin, and has been attributed to the "toughening" effect caused by Ca^{2+} rebinding and the corresponding crosslinking process.[28] However, that cannot be the only factor, as such rebinding is not possible for chemical alginate gels. We argue that the discrepancy between the theoretical and experimental values are likely due to the change in chain density because of solvent transport in the stressed zone under the needle. Also,

the estimate of areal chain density may increase if a larger stressed-zone or cohesive zone is considered. However, a further theoretical investigation is needed.

Concluding remarks

In summary, nonlinear mechanical behavior of ionic and chemical alginate hydrogels have been investigated using shear and cavitation rheometry. Ionic alginate gels were prepared by adding calcium ions into an aqueous solution of alginate, and chemical alginate gels were synthesized through amide bond formation using a diamine crosslinker. The small-angle X-ray scattering results indicate that the local structure of chemical alginate gels remains unchanged with changing AAD concentration, whereas scattering profile in ionic alginate gels changes, particularly because of change in the junction zones diameter with increasing calcium concentration.

Large amplitude oscillatory shear experiments were conducted to characterize the nonlinearity of the material. Both ionic and chemical alginate gels display strain stiffening behavior at large strain, whereas, for the ionic alginate gels the onset of strain-stiffening takes place at a lower strain. The strain-stiffening behavior is followed by the cohesive failure in chemical alginate gels, whereas in ionic alginate gels the samples detach from the rheometer plate because of adhesive failure. In addition, in conjunction with the strain-stiffening behavior, both ionic and chemical alginate gels exhibit negative normal stress, primarily attributed to the deformation of semiflexible alginate chains rather than the bending and stretching of junction zones in ionic alginate gels. To capture the failure behavior, we further tested defect growth in these gels through the cavitation rheometry. We found that the fracture mechanism is different in ionic and chemical gels. For example, in chemical alginate gels, fracture propagates in a 2D circular shape and remains unaltered with changing AAD concentration. Conversely, the defect growth in ionic alginate gels is more 3D and its shape depends on the calcium concentration. Critical energy release rate, G_c, has been determined from the experimental results and also has been estimated from the classical LT theory. The experimentally determined G_c has been found to vary with the crosslinker concentration in the ionic gels. Whereas, in the chemical gels,G_c value is almost independent of the crosslinker concentration. The theoretically predicted values of G_c have been found to be significantly lower than that obtained experimentally likely due to the unaccounted factors in the LT theory and needs to be further explored in the future.

Acknowledgements

We acknowledge support from the National Science Foundation through CAREER award, DMR 1352572.

References

1 J. Elisseeff, K. Anseth, D. Sims, W. McIntosh, M. Randolph and R. Langer, *Proc. Natl. Acad. Sci.*, 1999, **96**, 3104–3107.
2 A. Lueckgen, D. S. Garske, A. Ellinghaus, R. M. Desai, A. G. Stafford, D. J. Mooney, G. N. Duda and A. Cipitria, *Biomaterials*, 2018, **181**, 189–198.
3 E. A. Appel, M. W. Tibbitt, M. J. Webber, B. A. Mattix, O. Veiseh and R. Langer, *Nat. Commun.*, 2015, **6**, 6295.
4 H. Yuk, T. Zhang, G. A. Parada, X. Liu and X. Zhao, *Nat. Commun.*, 2016, **7**, 12028.
5 C. Storm, J. J. Pastore, F. C. MacKintosh, T. C. Lubensky and P. A. Janmey, *Nature*, 2005, **435**, 191–194.
6 Q. Wen, A. Basu, J. P. Winer, A. Yodh and P. A. Janmey, *New J. Phys.*, 2007, **9**, 428.
7 S. M. Hashemnejad and S. Kundu, *J. Polym. Sci. Part B Polym. Phys.*, 2016, **54**, 1767–1775.
8 P. A. Janmey, M. E. McCormick, S. Rammensee, J. L. Leight, P. C. Georges and F. C. MacKintosh, *Nat. Mater.*, 2007, **6**, 48–51.
9 A. V. Dobrynin, J.-M. Y. Carrillo and M. Rubinstein, *Macromolecules*, 2010, **43**, 9181–9190.
10 N. A. Kurniawan and C. V. C. Bouten, *Extreme Mech. Lett.*, 2018, **20**, 59–64.
11 A. R. Cioroianu and C. Storm, *Phys. Rev. E*, 2013, **88**, 052601.
12 F. Meng and E. M. Terentjev, *Soft Matter*, 2016, **12**, 6749–6756.
13 T. Yamamoto, Y. Masubuchi and M. Doi, *ACS Macro Lett.*, 2017, **6**, 512–514.
14 C. J. Kearney, H. Skaat, S. M. Kennedy, J. Hu, M. Darnell, T. M. Raimondo and D. J. Mooney, *Adv. Healthc. Mater.*, 2015, **4**, 1634–1639.
15 O. Smidsrød, *Faraday Discuss. Chem. Soc.*, 1974, **57**, 263–274.
16 R. Wijayapala, S. M. Hashemnejad and S. Kundu, *RSC Adv.*, 2017, **7**, 50389–50395.
17 J. A. Zimberlin, N. Sanabria-DeLong, G. N. Tew and A. J. Crosby, *Soft Matter*, 2007, **3**, 763–767.
18 S. Kundu and A. J. Crosby, *Soft Matter*, 2009, **5**, 3963–3968.
19 S. M. Hashemnejad and S. Kundu, *Soft Matter*, 2015, **11**, 4315–4325.
20 S. Mishra, T. E. Lacy and S. Kundu, *Int. J. Non-Linear Mech.*, 2018, **98**, 23–31.
21 S. M. Hashemnejad and S. Kundu, *Langmuir*, 2017, **33**, 7769–7779.
22 S. M. Hashemnejad, M. M. Huda, N. Rai and S. Kundu, *ACS Omega*, 2017, **2**, 1864–1874.
23 K. C. Bentz, N. Sultan and D. A. Savin, *Soft Matter*, 2018, **14**, 8395–8400.
24 R. H. Ewoldt, A. E. Hosoi and G. H. McKinley, *J. Rheol.*, 2008, **52**, 1427–1458.
25 J. Ilavsky, F. Zhang, R. N. Andrews, I. Kuzmenko, P. R. Jemian, L. E. Levine and A. J. Allen, *J. Appl. Crystallogr.*, 2018, **51**, 867–882.
26 B. T. Stokke, K. I. Drager, Y. Yuguchi, H. Urakawa and K. Kajiwara, *Macromol. Symp.*, 1997, **120**, 91–101.
27 Y. Yuguchi, A. Hasegawa, A. M. Padoł, K. I. Draget and B. T. Stokke, *Carbohydr. Polym.*, 2016, **152**, 532–540.
28 T. Baumberger and O. Ronsin, *J. Chem. Phys.*, 2009, **130**, 061102.
29 X. Zhao, N. Huebsch, D. J. Mooney and Z. Suo, *J. Appl. Phys.*, 2010, **107**, 063509.
30 J. Kang, C. Wang and H. Tan, *Soft Matter*, 2018, **14**, 7979–7986.
31 W.-C. Lin, W. Fan, A. Marcellan, D. Hourdet and C. Creton, *Macromolecules*, 2010, **43**, 2554–2563.
32 R. Bai, Q. Yang, J. Tang, X. P. Morelle, J. Vlassak and Z. Suo, *Extreme Mech. Lett.*, 2017, **15**, 91–96.
33 C. K. Roy, H. L. Guo, T. L. Sun, A. B. Ihsan, T. Kurokawa, M. Takahata, T. Nonoyama, T. Nakajima and J. P. Gong, *Adv. Mater.*, 2015, **27**, 7344–7348.

34 S. Mishra, R. M. B. Prado, T. E. Lacy and S. Kundu, *Soft Matter*, , DOI:10.1039/C8SM01397G.
35 Y. Y. Lin and C. Y. Hui, *Int. J. Fract.*, 2004, **126**, 205–221.
36 G. J. Lake and A. G. Thomas, *Proc R Soc Lond A*, 1967, **300**, 108–119.
37 P. Agulhon, V. Markova, M. Robitzer, F. Quignard and T. Mineva, *Biomacromolecules*, 2012, **13**, 1899–1907.
38 H. J. Kong, E. Wong and D. J. Mooney, *Macromolecules*, 2003, **36**, 4582–4588.

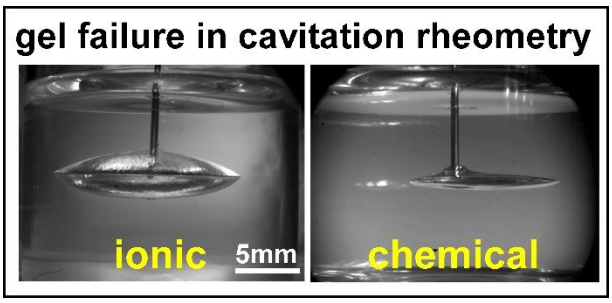

Non-linear rheological properties and failure behavior of ionic and chemically crosslinked alginate hydrogels are investigated